ANALYSIS OF EFFECTS OF THE FREE SURFACE ON THE MOVEMENT OF A TETHERED SPHERE IMMERSED IN A STEADY FLOW

D. Mirauda
D. Mirauda, Department I.F.A., Basilicata University, Viale dell'Ateneo Lucano, Potenza, Italy

S. Malavasi
S. Malavasi, Department I.I.A.R., Politecnico di Milano, Piazza L. da Vinci 32, Milano, Italy

A. Volpe Plantamura
A. Volpe Plantamura, Department I.F.A., Basilicata University, Viale dell'Ateneo Lucano,Potenza, Italy

ABSTRACT

In this work, we study the effects of the free surface on the sphere immersed in a steady flow through the analysis of stream wise and transverse displacements. The range of relative submergence, h, is between 0 and 0.75 and the tethered sphere is characterized by a low value of the mass ratio m*~1 and a low value of damping ratio (ζ=0.007). The movements of the sphere have been measured using two methods: (a) by means of an analogue laser displacement sensor, and (b) by image analysis of the sphere movement CCD acquisitions. The second method provided the 2D reconstruction of the trajectory. The experimental data have highlighted a significant influence of free surface flow both on the transverse oscillation amplitudes and on the oscillation frequencies of the sphere.*

1. INTRODUCTION

The problem of vortex-induced vibration of structures is important in many fields of engineering. This has led to a large number of fundamental studies that are summarized in the comprehensive reviews of Sarpkaya (1979), Griffin and Ramberg (1982), Bearman (1984), Parkinson (1989) and Williamson and Govardhan (2004) and the books by Blevins (1990), Naudascher and Rockwell (1994), Sumer and Fredsoe (1997) and Anagnostopoulos (2002). Most of these studies have been on cylindrical structures, and prior to some preliminary work (Govardhan and Williamson, 1997, 2005; Jauvtis et al., 2001; Mirauda et al., 2004, 2007; Greco et al. 2005) there is almost no reported work on vortex-induced vibrations of a sphere despite its practical significance. Some practical examples include tethered bodies like marine buoys, underwater mines, tethered balloons in the atmosphere, and towed object behind ships.

In the present work, we seek to understand the influence of free surface flow on the amplitude and frequency response of a tethered sphere free to move in both the stream wise and transverse directions to the fluid flow, for determined values of mass and damping ratios.

The studies, developed in the last years on the flow-sphere interaction (Govardhan and Williamson, 1997, 2005; Jauvtis et al., 2001; Mirauda et al., 2004, 2007; Greco et al., 2005), highlight the existence of a significant dependence of the transverse and stream wise oscillation amplitudes, A^*_y and A^*_x, and of the transverse frequency ratio, f*, in function of normalized velocity, U*, changing mass, damping ratio and relative submergence (see Table 1).

Jauvtis et al. (2001), analyzing the vibrations of tethered spheres free to move in both stream wise and transverse directions to flow for high values of relative submergence (h*>>1) and for a very wide range of normalized velocities (U* = 0 – 300), find three different modes of response (Figure 1 and 2). The first two modes observe in the case of a sphere immersed in a water flow for values of m* from 0.8 to 28, while the third mode in the case of sphere in wind tunnels around to values U* of about 20 and for mass ratios of 80 and 940. The Mode I response, that represents the origin of the synchronization regime, is characteristic of a resonance condition at U* = 6, and corresponds to the static body vortex shedding frequency lying close to the natural frequency and to the oscillation frequency of the body (Figure 3). The Mode II observes for normalized velocities between 8 and 15, where the body oscillation frequency is close to the static body vortex shedding frequency (Figure 3) and periodic vibrations occurs with large amplitudes close to one diameter. For the high-speed (U*>20) the Mode III observe where the body dynamics cannot be synchronised with the principal vortex shedding frequency. In fact the principal vortex shedding frequency is from 3 to 8 times the body oscillation frequency and so the classical lock-in or synchronization of frequencies cannot explain this vibration mode.

Added mass	$m_a = 1/6 \cdot C_A \pi \rho D^3$
Mass ratio	$m^* = m/\pi\rho D^3/6$
Damping ratio	$\varsigma = c/2\sqrt{k(m+m_a)}$
Relative submergence	$h^* = h/D$
Transverse amplitude ratio	$A_y^* = \sqrt{2}y_{rms}/D$
Stream wise amplitude ratio	$A_x^* = \sqrt{2}x_{rms}/D$
Normalized velocity	$U^* = U/f_N D$
Transverse frequency ratio	$f^* = f/f_N$
Reynolds number	$\mathrm{Re} = \rho UD/\mu$
Froude number	$Fr = U/\sqrt{gD}$

where C_A = potential added mass coefficient (C_A = 0.5 for a sphere), m = sphere mass, c = structural damping, k = spring constant, h = distance from the free surface to the surface of the sphere, y_{rms} = root mean square of transverse oscillation amplitudes, x_{rms} = root mean square of stream wise oscillation amplitudes, f_N = mechanical natural frequency in the medium, D = sphere diameter, ρ = fluid density, U = free-stream velocity, μ = fluid dynamic viscosity, f = oscillating frequency of the sphere, g = gravity acceleration, f_{vo} = non-oscillating body vortex shedding frequency.

Table 1: Non dimensional groups used.

Subsequently Govardhan and Williamson (2005) confirm the results of Jauvtis et al. (2001) relative to modes I and II and find the Mode III also for spheres in water channel. Such mode of response appears at high water flow velocities where the frequency of vibration is far below the frequency of vortex shedding for a static body. They note that the Mode II and Mode III regimes are always separated by a desynchronized region. Moreover, considering the stream wise response amplitudes of a sphere in function of U*, they observed a certain difference with transverse oscillations (Figure 4). In detail, the stream wise amplitude (A^*_x) are dependent from the mass ratio for sufficiently small mass, m*<6, while for larger sphere mass, m*>6, the stream wise can be considered negligible. Besides, for low mass ratio, it is possible to observe two type of oscillation trajectory: for m*<1 (the sphere is defined light) it is that an eight; while for m*>1 (the sphere is defined heavy) it is that of crescent topology (Figure 5).

In a different way respect to Jauvtis et al. (2001) and Govardhan and Williamson (2005), Mirauda et al. (2004, 2007) and Greco et al. (2005), analyzing the vibrations of a tethered sphere free to move in both stream wise and transverse directions to flow for low values of relative submergence (h*<1), for values of m* close to unity and for the a little range of normalized velocities investigated (U* = 0 – 8), reveal the only presence of the Mode I (Figure 1), with a crescent behaviour similar to the data of the previous Authors.

In the present work we reported the first results obtained analyzing the effects of the free surface on an tethered sphere in a steady flow through the measurement displacements. Follow a description of the experimental details and the discussion of the results.

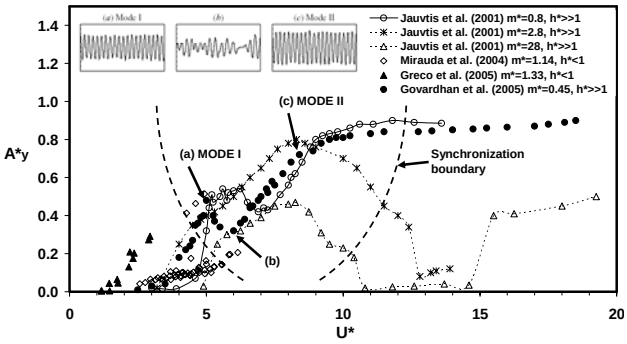

Figure 1: *Transverse amplitude ratio versus U*, for spheres with different m* and h* in water.*

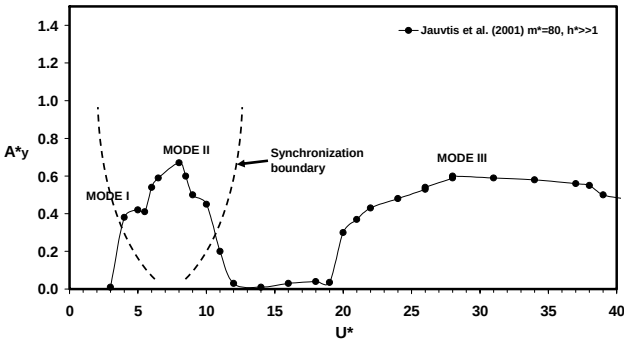

Figure 2: *A^*_y versus U*, for an heavy sphere in air.*

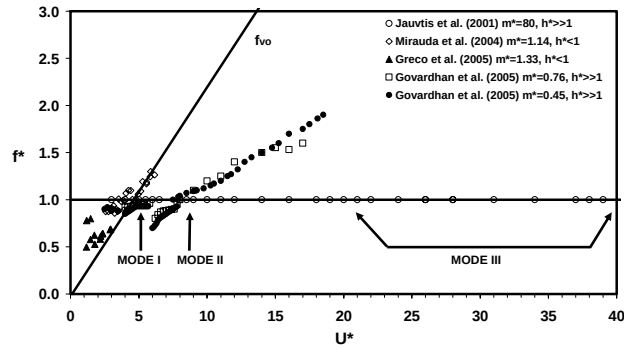

Figure 3: *Transverse frequency ratio versus U*, for spheres with different m* and h*, in air and water.*

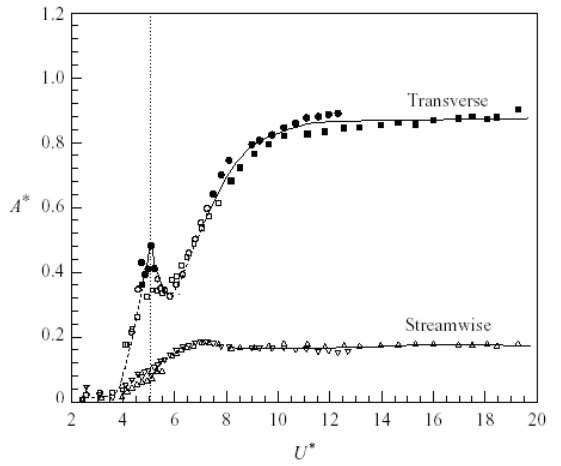

Figure 4: *Transverse and stream wise amplitudes versus U*, for a tethered sphere with m*=0.45, at different Re and lengths of the rod, in water.*

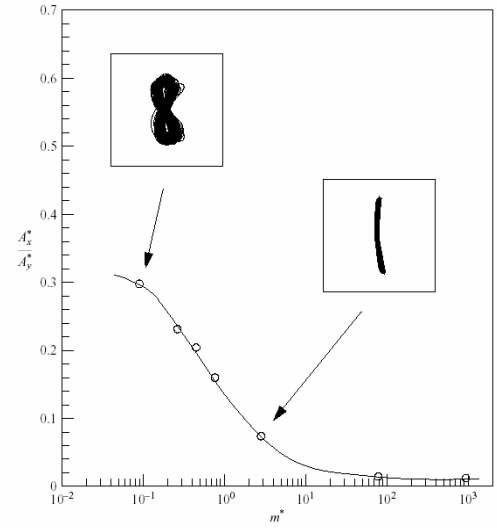

Figure 5: *Normalized stream wise amplitude (A^*_x/A^*_y) versus m*, for different tethered spheres.*

2. EXPERIMENTS

The experiments have been performed in a non-tilted Plexiglas open water channel with rectangular cross section, 0.6 m height, 0.5 m width and 5.0 m length. The obstacle used has been a water filled sphere with a diameter D=0.087 m. The sphere surface is made of PVC and covered with an episodic paint to reduce the surface roughness. A rod has been used to connect the sphere to a fixed structure. The rod is made of stainless steel and Derlin. The stainless steel part, which is connected to the sphere, is 0.080 m long and 3 mm in diameter. The Derlin part completes the rod with a diameter of 12 mm. The distance between sphere and channel floor has been set at 3 mm. Figure 6 shows the sketch of the obstacle rest.

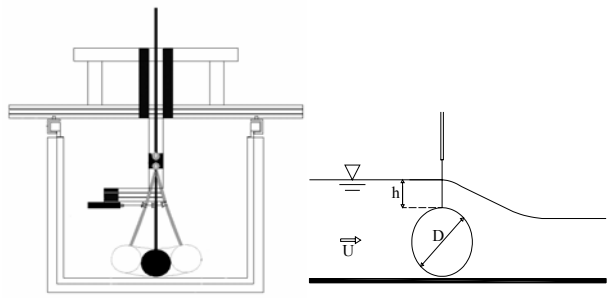

Figure 6: *Sketch of the obstacle rest mounted on the channel (cross-section).*

The movements of the sphere have been measured using two methods: an analogue laser displacement sensor able to provide only the transverse displacements and an image analysis of CCD (Charge Coupled Device) acquisitions, able to provide the 2D (stream wise and transverse) displacements of the sphere. With the two techniques of displacement measure it has been possible to elaborate a spectral analysis of the signal, from which have been deduced the transverse oscillation frequencies useful for the analysis of the results.

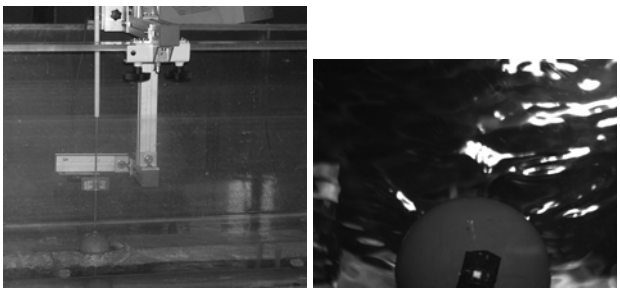

(a) *(b)*

Figure 7: *Two different techniques of displacement measure: a) laser sensor; (b) view of marker by CCD camera.*

Table 2 summarized the experimental range considered in this work. The measurements have been taken for many different steady flows produced ($0.2 < U < 0.8$ m/s). All the generated steady flows ranging from 0.22 to 0.87 of Froude number; from $1.74 \cdot 10^4$ to $6.96 \cdot 10^4$ of Reynolds number and are run for relative submergence from h*=0 to h*=0.75.

U (m/s)	h*	Fr	Re	ζ	f_n (Hz)
0.2	0 – 0.75	0.22	$1.74 \cdot 10^4$	0.007	1.57 - 1.51
0.3	0 – 0.75	0.32	$2.61 \cdot 10^4$	0.007	1.57 - 1.51
0.4	0 – 0.75	0.43	$3.48 \cdot 10^4$	0.007	1.57 - 1.51
0.5	0 – 0.75	0.54	$4.35 \cdot 10^4$	0.007	1.57 - 1.51
0.6	0.16 – 0.75	0.65	$5.22 \cdot 10^4$	0.007	1.56 - 1.51
0.7	0.31 – 0.75	0.76	$6.09 \cdot 10^4$	0.007	1.54 - 1.51
0.8	0.75	0.87	$6.96 \cdot 10^4$	0.007	1.51

Table 2: The characterized size of the investigated steady flow.

To compare the transverse displacements obtained with the two techniques, it is made necessary to report both the movements to an only system of reference that has its origin in the centre of the sphere. To bring the displacements by CCD camera to the new system of reference has been calculated in a first moment the inclination of the rod for every measure through a simple trigonometric relationship of the type:

$$\alpha = arctg\left(\frac{y_{rms}}{H_{rod} + D}\right) \quad (1)$$

in which α is the inclination of the rod, y_{rms} is the root mean square of signal by CCD camera, and H_{rod} is the height of rod (Figure 8). Subsequently, the root mean square of signal has been multiplied for the tangent of α. These movements of the CCD camera have been reported on a graph with those acquired by the sensor, and, by best-fit line, has been calculated the difference in percentage among the two movements. The real movements of the sphere centre have been obtained multiplying the value of the angular coefficient of best-fit line for displacements measured by the sensor. The comparison among this last ones and those measured by the CCD camera has given a error lower than 10% for almost all the displacements, underlining the precision of the two techniques of measures (Figure 8). Such precision has been confirmed, besides, from the analysis of the oscillation frequencies obtained by the power spectrum. As it possible to observe by an example reported in Figure 9, the frequencies of oscillation result equal for the two techniques.

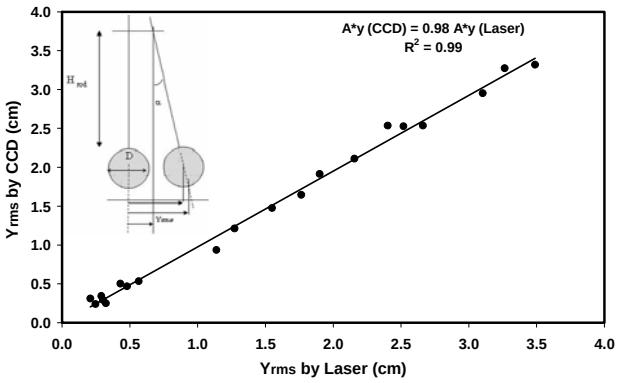

Figure 8: *Displacements of the sphere centre with the two techniques.*

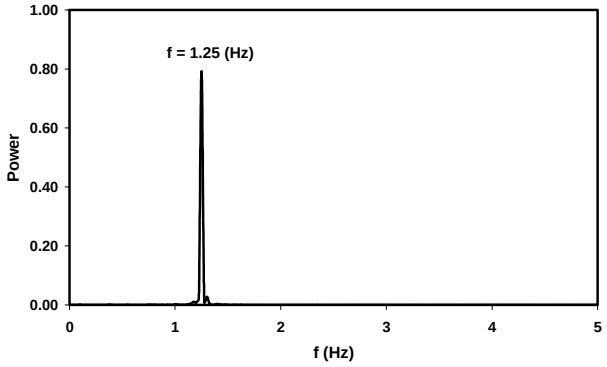

(a)

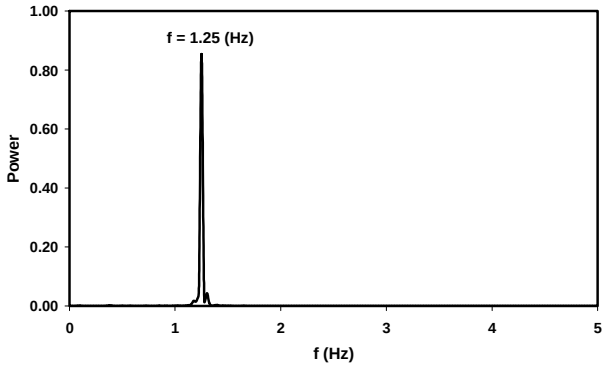

(b)

Figure 9: *Power spectrum of signal for U*=1.72, h*=0.16: (a) by laser sensor; (b) by CCD camera.*

3. RESULTS

As mentioned above, the maximum amplitude of a structure depends from the normalized velocity, therefore plotting the transverse amplitude versus U* (Figure 10) it is possible to observe how our system reproduces in a very similar manner, for all the different values of h*, the curve of Jauvtis et al. (2001) also if it is translated to left and with amplitudes reduced. More in detail, the synchronization regime is reached for values of U* lower than those found from others Authors

obtained for spheres fully submerged. This could be due at the formation of jet-like flow between upper surface of the sphere and the free surface, characterized by a very low-velocity region of quiescent fluid that slow down the vibrations of the body. Besides, it doesn't observe the peak response amplitude that is characteristic of resonance condition because the presence of free surface near to the sphere conditions the dynamic of body reducing both the oscillation amplitudes and frequencies. The same result is evident by diagram of f* in function of U* (Figure 11), where the motion evolves close to the Mode I of response, reaching the synchronization regime but not the resonance condition (f^*=1).

As already described by Govardhan and Williamson (2005) for low mass ratios, it is possible to note also the presence of a region of non-periodic response within of the synchronization regime (Figure 1). According with those observed by the authors, Figure 12 reports the time-history of the transverse displacements of some data plotted in Figure 10. The points marked with 1, 3 and 5 show a periodic trend typical of the Mode I, while the points 2, 4 and 6 show a random component in the trend typical of the transition between two modes (Mode I and Mode II) as reported in Figure 1.

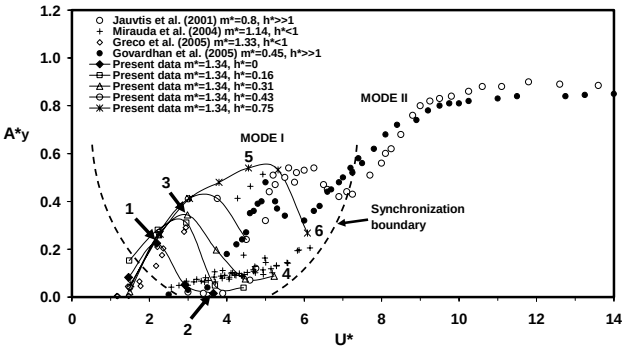

Figure 10: *Transverse amplitude ratio versus U*, for spheres with low m*, in water.*

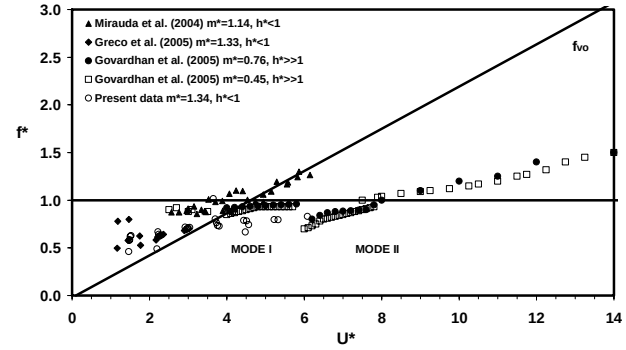

Figure 11: *Transverse frequency ratio versus U*, for spheres with low m*, in water.*

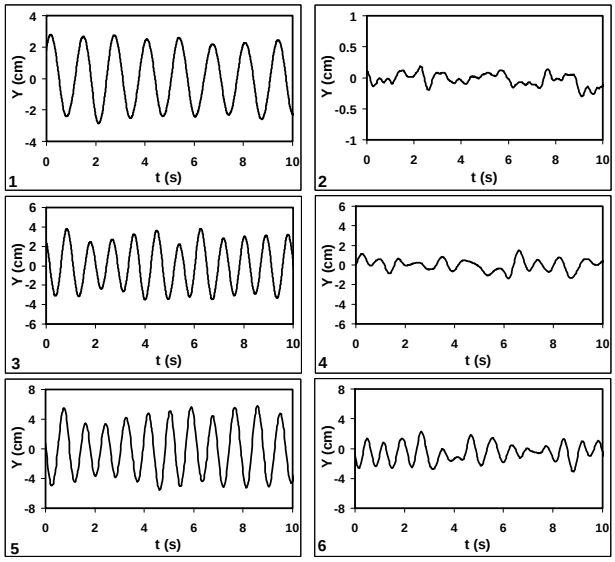

Figure 12: *Transverse movements of the sphere in the time.*

Finally, as discussed first, the stream wise oscillations of the sphere could not influence the dynamic response of the body, therefore, in Figure 13 we report a direct comparison between transverse and stream wise amplitudes in function of U*. The data points confirm the tendency found by Govardhan and Williamson (2005), in fact the transverse oscillation amplitudes are always predominant respect to those in stream wise direction, which are close to zero value, and this is confirmed by the use of CCD camera that has allowed to measure the trajectory of the movements on the horizontal plane of the sphere. As it is possible note from the Figure 14 the trajectory of displacements is that typical of crescent topologies. These results seem to agree with data of Govardhan and Williamsom (2005) obtained for values of m*> 1.

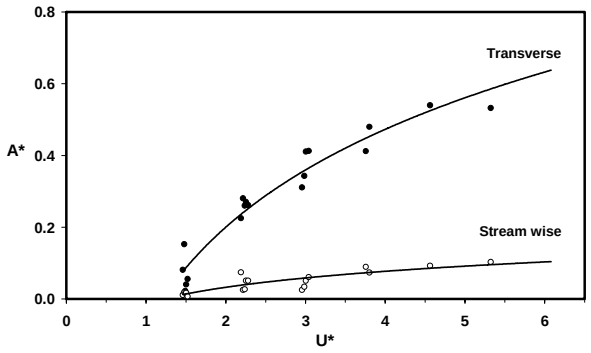

Figure 13: *Transverse and stream wise oscillation amplitude versus U*, for sphere with m*=1.34.*

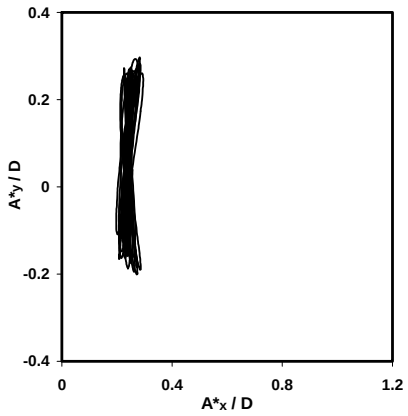

(a)

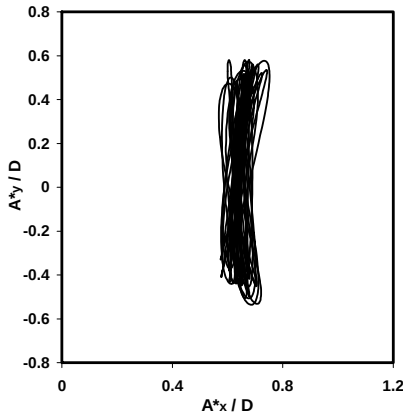

(b)

Figure 14: *Oscillation trajectories for h*=0.31: (a) U*=1.49; (b) U*=2.99.*

4. CONCLUSION

An experimental apparatus has been designed to study the flow field and the movements of a tethered sphere characterized by low value of relative submergence and low value of the mass and damping ratios.

The analysis of displacements leads to the following major results:

1. the comparison of transverse amplitudes obtained both with laser sensor and with CCD camera has given a error lower than 10%, underlining the precision of the two techniques of measure;
2. the synchronization regime is reached for values of U* lower than those found from others Authors for spheres fully submerged, but it isn't reached the resonance condition;
3. it is possible to note the presence of a region of non-periodic response within of the synchronization regime;
4. the trajectory of the movements on the horizontal plane of the sphere is that typical of crescent topologies for m*>1.

5. REFERENCES

Govardhan, R., and Williamson, C.H.K., 1997, Vortex induced motions of a tethered sphere. In *Journal of Wind Engineering and Industrial Aerodynamics*, **69-71**: 375-385.

Govardhan, R., and Williamson, C.H.K., 2005, Vortex induced vibration of a sphere. In *Journal of Fluid Mechanics*, **531**: 11-47.

Greco, M., et al.**,** 2005, Interaction between a tethered sphere and a free surface flow. In *Fluid Structure Interaction and Moving Boundary Problems* (eds S.K. Chakrabarti, S. Hernandez & C.A. Brebbia), **84**: 205-213. WitPRESS.

Jauvtis, N., et al. 2001, Multiple modes of vortex-induced vibration of a sphere. In *Journal of Fluids and Structures*, **15**: 555-563.

Mirauda, D., and Greco, M., 2004, Flow-induced vibration of an elastically sphere at high combined mass-damping parameter. In *Journal of IASME Transactions,* **1**: 486-491.

Mirauda, D., and Greco, M., 2004, Transverse vibrations of an sphere at high combined mass-damping parameter. Shallow Flows (eds G. H. Jirka & W.S.J. Uijttewaal) 111-115. Balkema Publisher.

Mirauda, D., et al., 2007, Kinematic analysis of the movement of a tethered sphere immersed in a free surface flow. 9th Intl. Symp. Fluid Control, Measurement and Visualization, Flucome 2007, Paper 151, Tallahassee, FL (CD-Rom).